MEMOIRS OF THE FACULTY OF SCIENCE, KYOTO UNIVERSITY, SERIES OF BIOLOGY
Vol. IX, pp. 97–105, October 1984

Helmholtz-Type Equation with Fixed Boundary May Predict the Position of the Division Plane and the Direction of the Spindle Axis

By

HIROFUMI DOI

Department of Biophysics, Faculty of Science, Kyoto University, Kyoto, 606 Japan

(Received March 30, 1984)

Abstract. Helmholtz-type equation with fixed boundary was solved numerically in regard to the squashed sea urchin egg cell by cell. The results suggest that the equation may predict the direction of the spindle axis and the position of the division plane.

1. Introduction

What does determine the cleavage pattern? This is one of the greatest problems in developmental biology. Birds, fishes, snakes and others usually show cleavage pattern called discoidal cleavage. Fig. 1a shows the standard beautiful pattern of discoidal cleavage up to the 16-cell stage (Patten and Carlson, 1974; Ham and Veomett, 1980). Fig. 1b shows the eigenfunctions of the following Helmholtz-type equation (Mizumoto, 1973):

$$(\partial^2/\partial x^2+\partial^2/\partial y^2)u=-\lambda u \tag{1}$$

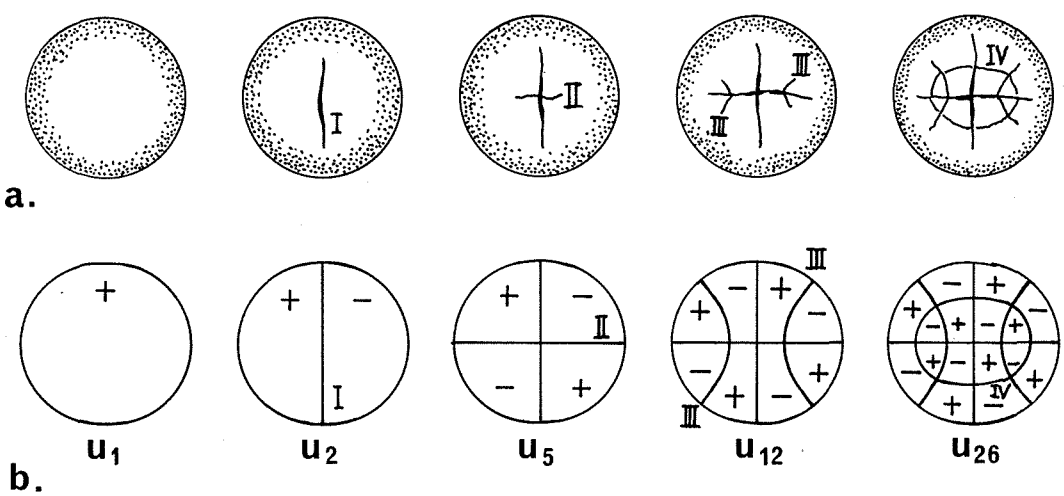

Fig. 1. a, the standard beautiful discoidal cleavage pattern (redrawn from Patten and Carlson, 1974); b, the eigenfunctions of eq. (1) with an almost circular ellipse (redrawn from Mizumoto, 1973).

with the fixed boundary condition

$$u=0 \quad \text{on} \quad \partial\Omega,$$

where Ω is an almost circular ellipse and $\partial\Omega$ is its boundary.

Comparing these figures we notice that there is a close similarity between Fig. 1a and b. The nodal lines I,..., IV in Fig. 1b correspond to the cleavage lines I,..., IV in Fig. 1a, respectively. From this fact we may well have the following question extended three dimensionally:

Are there any relationship between the cleavage pattern and the following equation?

$$(\partial^2/\partial x^2+\partial^2/\partial y^2+\partial^2/\partial z^2)U=-\mu U \tag{2}$$

with the boundary condition

$$U=0 \quad \text{on} \quad \partial\Omega_0,$$

where Ω_0 is a three-dimensional domain and $\partial\Omega_0$ is its boundary.

I attempted to solve eq. (2) with regard to a living egg, but it is difficult to solve eq. (2) as it is, so eq. (2) is put in two-dimensional, i.e. eq. (1), and solved with regard to the cleavage pattern of a squashed sea urchin egg. This paper presents the results.

2. Preliminary theory

From many isolated blastomere experiments E. B. Wilson (1904) had concluded that the cell develops independent of the other cells. So, when we consider the similarity, it might be adequate that we consider the Laplacian not to operate in a whole embryo but in a component cell. We solve eq. (2) separately with regard to each cell boundary, then every cell has the individual solutions of eq. (2). And if the cell divided, two new cell boundaries are formed, we solve eq. (2) with each new boundary. That is, eq. (2) is solved cell by cell. In case of an ellipse, the eigenfunction for the second eigenvalue of eq. (1) has one nodal line and this ellipse is divided into two halves (Fig. 1b). Thus we hypothesize as follows:

(H) A dividing cell (Ω_0 is its three-dimensional shape) cleaves along the nodal plane $U_2=0$ of eq. (2), where U_2 is the eigenfunction for the second eigenvalue.

The i-th eigenvalue of eq. (2) (i=1, 2,...) is denoted by μ^i and the eigenfunction for μ^i (the i-th mode) by U_i. With regard to eq. (1), in the same way, its i-th eigenvalue is denoted by λ^i and the eigenfunction for λ^i (the i-th mode) by u_i. Here $\mu^1\leqq\mu^2\leqq\cdots$ and $\lambda^1\leqq\lambda^2\leqq\cdots$.

When Ω_0 is a pillar with an altitude L_z long and the base Ω, where Ω is a two-dimensional shape on x−y plane (Fig. 2, we call this pillar an Ω-pillar), we separate the variables of U(x, y, z) as follows:

$$U=u(x, y)v(z).$$

Eq. (2) is represented as follows:

$$\begin{cases} (\partial^2/\partial x^2+\partial^2/\partial y^2)u=-\lambda u \quad (u=0 \quad \text{on} \quad \partial\Omega) & (3)\\ d^2v/dx^2=-\lambda_z v \quad (v=0 \text{ at } z=0 \text{ and } L_z) & (4)\\ \mu=\lambda+\lambda_z & (5) \end{cases}$$

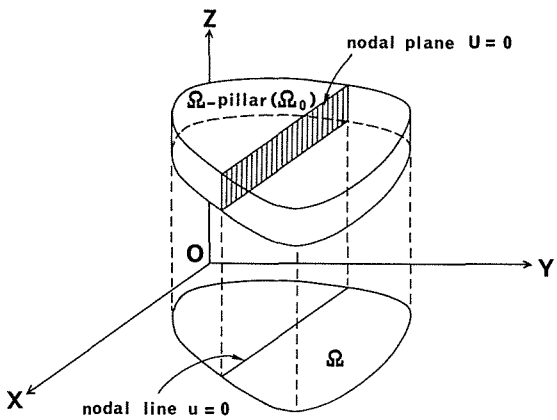

Fig. 2. The nodal plane U=0 of an Ω-pillar (Ω_0) and the nodal line u=0 of Ω. The projection of the nodal plane to x–y plane is the nodal line. See text.

Eq. (3) is just the same as eq. (1). Moreover, if Ω_0 is flat, then there is a positive integer I (>2) such that

$$\begin{cases} \mu^i=\lambda^1+\lambda_z^1 & (i\leqq I-1) \quad (6) \\ \mu^I=\lambda^1+\lambda_z^2 & (7) \end{cases}$$

where $\lambda_z^k=(k\pi/L_z)^2$ (k=1, 2). The smaller L_z is, the bigger λ_z^2 is. In other words, the flatter Ω_0 is, the bigger I is. For example, when Ω_0 is a rectangular parallelepiped with a height three long, a width five long and a depth two long, I equals eight, i.e. $\mu^8>\mu^i$ (i=1,..., 7; see Table 1). The nodal plane of the i-th mode ($U_i=0$) of eq. (2) is perpendicular to x—y plane. Its projection to x—y plane coincides with the nodal line of the i-th mode ($u_i=0$) of eq. (1) (Fig. 2). When Ω_0 is a flat Ω-pillar, therefore, to look for the nodal plane $U_i=0$ is reduced to do the nodal line $u_I=0$, i.e., to solve eq. (1).

Thus when Ω_0 is flat, we may put the hypothesis (H) in two dimensional.

Table 1. The eigenvalues of eq. (2) with the rectangular parallelepiped in text.

i	1	2	3	4	5
λ_x^i/π^2	1/25	4/25	9/25	16/25	25/25
λ_y^i/π^2	1/9	4/9	9/9	16/9	25/9
λ_z^i/π^2	1/4	4/4	9/4	16/4	25/4

μ^i	μ^i/π^2	μ^i	μ^i/π^2
$\mu^1=\lambda_x^1+\lambda_y^1+\lambda_z^1$	361/900	$\mu^9=\lambda_x^2+\lambda_y^1+\lambda_z^2$	1144/900
$\mu^2=\lambda_x^2+\lambda_y^1+\lambda_z^1$	469/900	$\mu^{10}=\lambda_x^1+\lambda_y^3+\lambda_z^1$	1161/900
$\mu^3=\lambda_x^3+\lambda_y^1+\lambda_z^1$	649/900	$\mu^{11}=\lambda_x^4+\lambda_y^2+\lambda_z^1$	1201/900
$\mu^4=\lambda_x^1+\lambda_y^2+\lambda_z^1$	661/900	$\mu^{12}=\lambda_x^5+\lambda_y^1+\lambda_z^1$	1225/900
$\mu^5=\lambda_x^2+\lambda_y^2+\lambda_z^1$	769/900	$\mu^{13}=\lambda_x^3+\lambda_y^3+\lambda_z^1$	1269/900
$\mu^6=\lambda_x^4+\lambda_y^1+\lambda_z^1$	901/900	$\mu^{14}=\lambda_x^3+\lambda_y^1+\lambda_z^2$	1324/900
$\mu^7=\lambda_x^3+\lambda_y^2+\lambda_z^1$	949/900	$\mu^{15}=\lambda_x^1+\lambda_y^2+\lambda_z^2$	1336/900
$\mu^8=\lambda_x^1+\lambda_y^1+\lambda_z^2$	1036/900	$\mu^{16}=\lambda_x^2+\lambda_y^2+\lambda_z^2$	1444/900

3. Materials and methods

(1) Obtaining squashed cells

Gametes of the sea urchin *Hemicentrotus pulcherrimus* were obtained by injection of 0.5 M KCl. Eggs were collected in artificial sea water (Jamarin U) and washed several times to remove the jelly coats. Sperm was taken "dry" from excised testes, and diluted just before use. Eggs were fertilized and allowed to develop in artificial sea water. All experiments were performed at 18–19°C. To get squashed cells, glass-bars (about 35 μm in diameter) which act as spacers were placed on plate. A drop of egg suspension (at the streak stage) was placed among them and pressed with a coverslip. This preparation was sealed with liquid paraffin. Control eggs under the similar preparation with glass-bars of about 150 μm in diameter showed normal development until at least blastula stage. Untreated control eggs developed at least Pluteus larva.

The development of a specified embryo, called embryo I, was recored on 16 mm color film with Nikon movie camera adapted for microscope (Oplympus, BH).

(2) Computation

Eq. (1) was solved numerically with the difference method. The boundary $\partial\Omega$ was obtained by approximating the observed cell boundary with mesh points. We use the cell boundaries of embryo I just before cytokinesis. The mesh size is (30/6.2) μm to the cells at the two-cell stage and (20/6.2) μm to those at the four- and eight-cell stages. When the mesh is of these sizes, in solving eq. (1) with each cell boundary we may choose the coordinate system arbitrarily and independently of other cells in the embryo. For, when the mesh is of these sizes, the eigenvalues and the eigenfunctions little change by the rotation and the parallel

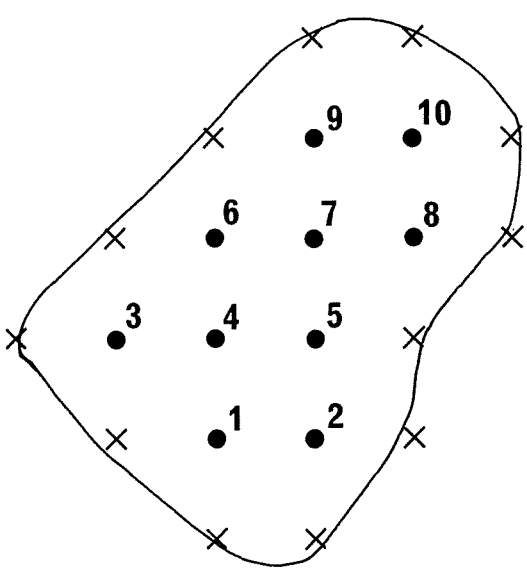

Fig. 3. An illustration to solve eq. (1) numerically. x, boundary mesh point; ●, inner mesh point.

translation of the coordinate system. Note: The rotation and the parallel translation of the coordinate system do not change the eigenvalues of eq. (1) and essentially even the eigenfunctions. This method transforms solving eq. (1) into searching for the eigenvalues and the eigenvectors of a matrix **D** with 0, 1, −4. For example, the matrix **D** to the figure and the mesh points in Fig. 3 equals to

	1	2	3	4	5	6	7	8	9	10
1	−4	1	0	1	0	0	0	0	0	0
2	1	−4	0	0	1	0	0	0	0	0
3	0	0	−4	1	0	0	0	0	0	0
4	1	0	1	−4	1	1	0	0	0	0
5	0	1	0	1	−4	0	1	0	0	0
6	0	0	0	1	0	−4	1	0	0	0
7	0	0	0	0	1	1	−4	1	1	0
8	0	0	0	0	0	0	1	−4	0	1
9	0	0	0	0	0	0	1	0	−4	1
10	0	0	0	0	0	0	0	1	1	−4

To solve eq. (1) in regard to this figure equals to do $\mathbf{Du}=-\lambda\mathbf{u}$, where $\mathbf{u}=(u^1, u^2,\ldots, u^{10})^T$ and u^i is the value of **u** at the i-th point (i=1, 2,..., 10). DSEIG2 (one of the scientific subroutines, SSL II, constructed by Fujitsu Co. and installed in Data Processing Center of Kyoto Univ.) computed the eigenvalues and the normalized eigenvectors of **D**. The computation results were displayed in the form of two-dimensional patterns on printer sheets such as Fig. 4a–d.

4. Results

(1) Comparison of λ_z and λ's

As the spacer diameter is about 35 μm, let $L_z=35$ (μm), then $\lambda_z^1=(\pi/35)^2$ (μm^{-2}) and $\lambda_z^2=(2\pi/35)^2$ (μm^{-2}), approximately $\lambda_z^1=0.80486\times10^{-2}$ and $\lambda_z^2=0.32195\times10^{-1}$. On the other hand, λ^i (i=1, 2,..., 5) of each cell of embryo I to the eight-cell stage are given in Table 2. From Table 2 and the values of λ_z^1 and λ_z^2, we can tell that the integer I (>5) exists, which satisfies equation (6) and (7), for each cell to the eight-cell stage. For $\lambda^i<\lambda_z^2$ ($i\leqq I-1$) from equation (6) and (7), and the all eigenvalues in Table 2 are smaller than λ_z^2.

(2) General comments on the eigenfunctions

Fig. 4a and b show the sign and the magnitude of the normalized eigenfunction u_1 (the first mode) of cell-1 at the two-cell stage just before cytokinesis, respectively. Fig. 4c and d are of the second mode u_2 of the same cell, and Fig. 4e shows the A–B section of u_2. P and M in these figures indicate the maximum and the minimum points of the eigenfunctions, respectively. D denotes that the value u of the normalized eigenfunction at that point is smaller than 0.11 and

Table 2. The eigenvalues of eq. (1) with regard to each cell of embryo I up to the eight-cell stage. "E–4" denotes "10^{-4}", and "E–3" does "10^{-3}".

	2 cell stage		4 cell stage			
Cell	1	2	1	2	3	4
λ^1	0.26187E–4	0.28699E–4	0.53803E–4	0.47480E–4	0.52541E–4	0.51872E–4
λ^2	0.47539E–4	0.51163E–4	0.12299E–3	0.10621E–3	0.11100E–3	0.11015E–3
λ^3	0.73025E–4	0.79590E–4	0.13769E–3	0.12677E–3	0.14361E–3	0.13944E–3
λ^4	0.86879E–4	0.95108E–4	0.21216E–3	0.18023E–3	0.18690E–3	0.18594E–3
λ^5	0.10454E–3	0.11357E–3	0.24855E–3	0.22251E–3	0.23896E–3	0.23707E–3

	8 cell stage			
Cell	1	2	3	4
λ^1	0.13965E–3	0.11567E–3	0.95640E–4	0.12475E–3
λ^2	0.33808E–3	0.34173E–3	0.26930E–3	0.31197E–3
λ^3	0.33808E–3	0.34173E–3	0.26930E–3	0.31197E–3
λ^4	0.40816E–3	0.38162E–3	0.29446E–3	0.50489E–3
λ^5	0.48600E–3	0.49997E–3	0.38499E–3	0.52988E–3
Cell	5	6	7	8
λ^1	0.11636E–3	0.94537E–4	0.98330E–4	0.12237E–3
λ^2	0.25029E–3	0.19562E–3	0.18570E–3	0.26818E–3
λ^3	0.30207E–3	0.24322E–3	0.27213E–3	0.31056E–3
λ^4	0.43553E–3	0.32107E–3	0.32100E–3	0.47419E–3
λ^5	0.50235E–3	0.41820E–3	0.41144E–3	0.53542E–3

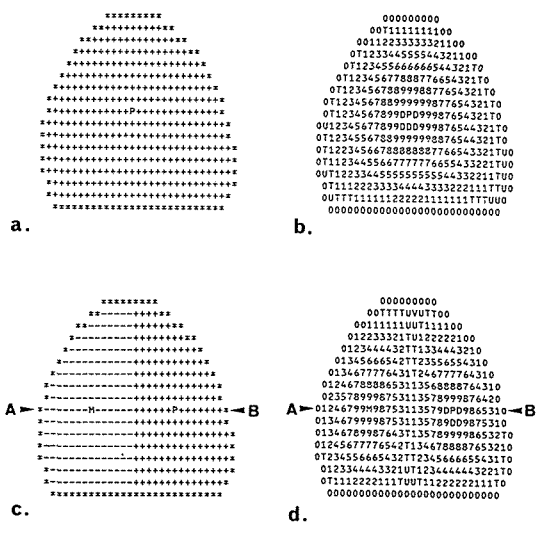

Fig. 4. The eigenfunctions of cell-1 at the two-cell stage of embryo I (see Fig. 5a and e). a, the sign b, the of u_1; magnitude of u_1; c and d, those of u_2, respectively; e, the A–B section of u_2.

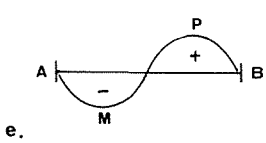

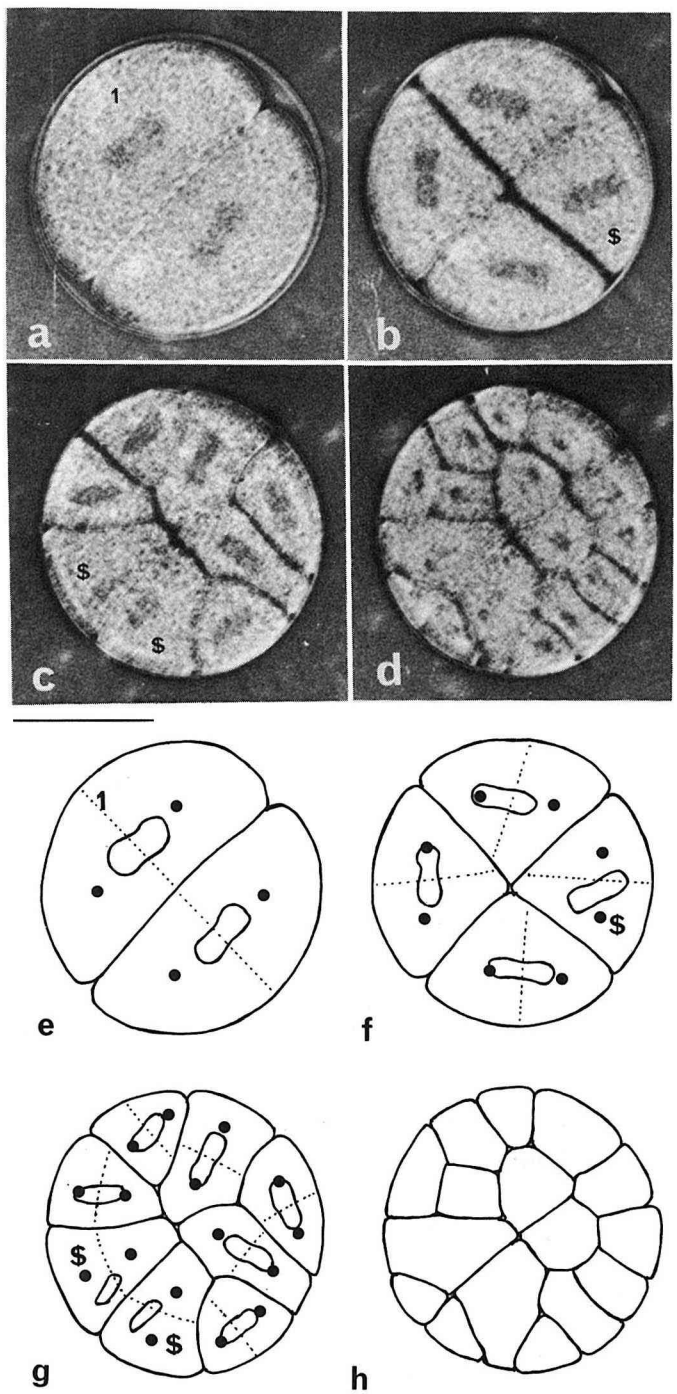

Fig. 5. a-d, the cleavage pattern of embryo I; e–h, the schematic diagrams; ●, the maximum and the minimum points of the second mode; the dotted line, the nodal line of the second mode. See text. Bar, 70 μm.

not smaller than 0.10, i.e., $0.11>|u|\geqq 0.10$. Similarly 9, $0.10>|u|\geqq 0.09$; 8, $0.09>|u|\geqq 0.008$; ...; 1, $0.02>|u|\geqq 0.01$; T, $0.01>|u|\geqq 0.005$; U, $0.005>|u|\geqq 0.001$; V, $0.001>|u|\geqq 0.0005$.

The first mode u_1 has only one mountain (plus area), and the second mode u_2 has one mountain and one conical valley (minus area). The nodal line of the second mode ($u_2=0$) is the boundary between them. The maximum point is the top of the mountain and the minimum point is the bottom of the valley. This fact is generally observed with the first and the second modes of every cell of embryo I.

We call the direction of line segments connecting the maximum and the minimum points of the second mode the max-min axis.

(3) Solutions of embryo I

Fig. 5a–d show the cleavage pattern of embryo I up to the 16-cell stage. These still pictures were printed from the 16 mm color film, so unsightly, but give the information about the direction of the spindle and the division pattern. In these pictures, the mitotic apparatus of each cell is seen as a black longitudinal zone. It was formed parallel to plate, and its axis coincides with the spindle axis.

At the fourth cleavage of the normal embryo, the four vegital blastomeres divide unequally into micromeres and macromeres. The similar phenomena also take place at the fourth cleavage of the squashed embryo (the two cells with \$; Fig. 5c).

Fig. 5e–h are the schematic diagrams of Fig. 5a–d. The nodal line and the max–min axis of the second mode of each cell is drawn in these schema according to the numerical solutions such as Fig. 4a–d. Except for the cells with \$, every cell forms the spindle of which axis almost agrees with the max–min axis of its second mode, and it seems to divide along the nodal line of the second mode.

5. Discussion

From the results we might conclude that: Helmholtz-type equation may predict the direction of the spindle and the division plane. But when a model supporting the results is devised, the following problem remains: What are the eigenfunction and the eigenvalue?

We get eq. (1) from both the wave equation and the diffusion equation by the variable-separation method. So when we regard u dynamically as the variable of the cytoplasm or some material, we think of the following non-linear wave equation:

$$\partial^2\tilde{U}/\partial t^2=f(\tilde{U})+c^2\Delta\tilde{U}$$

with the fixed boundary condition, where c is the spread velocity. While if u is the concentration of a diffusible material, we think of the following non-linear diffusion equation:

$$\partial\tilde{U}/\partial t=f(\tilde{U})+D\Delta\tilde{U}$$

with the Dirichlet boundary condition, where D is the diffusion constant. We also obtain eq. (1) as the equation of the steady state from these non-linear equation. In either case, however, we cannot interpret what λ is. We must find some phenomena which help us to

explain what u and λ are.

If u is the concentration of a diffusible material, the cell is not uniform in a strict sense. This is because it has the granules and vesicles in which the material cannot diffuse. We may disregard these obstacles whose sizes are smaller than the mesh size of the difference method. That is, even granules whose diameters are about 3 μm (see Materials and methods, (2) Computation) do not hinder the determination of the division plane.

In case of the curved boundary, the difference method is not so precise, compared with the finite element method (FEM). In addition a contour plot would give a more professional display of results such as those in Fig. 4. I am now under attempt to solve eq. (1) by FEM and to display results by a contour plot.

References

Mizumoto, H. (1973) Difference Method on Manifold. Kyoiku-Shuppan, Tokyo (in Japanese). 253 pp.

Patten, B. M. and B. M. Carlson (1974) Foundations of Embryology, 3rd ed. McGraw-Hill Book Co., New York.

Ham, R. G. and M. J. Veomett (1980) Mechanisms of Development. The C. V. Mosby Company, St. Louis. 843 pp.

Wilson, E. B. (1904) Experimental studies in germinal localization. J. Exp. Zool. 1: 197.